Journal of Magnetic Resonance **149,** 13–21 (2001)
doi:10.1006/jmre.2000.2277, available online at http://www.idealibrary.com on IDEAL®

Resonance-Field Dependence in Electrically Detected Magnetic Resonance: Effects of Exchange Interaction

Kôichi Fukui,*[,1] Toshiyuki Sato,† Hidekatsu Yokoyama,‡ Hiroaki Ohya,‡ and Hitoshi Kamada‡

*Regional Joint Research Project of Yamagata Prefecture, Matsuei 2-2-1, Yamagata 990-2473, Japan; †Yamagata Research Institute for Technology, Matsuei 2-2-1, Yamagata 990-2473, Japan; and ‡Institute for Life Support Technology, Yamagata Public Corporation for the Development of Industry, Matsuei 2-2-1, Yamagata 990-2473, Japan

Received June 12, 2000; revised December 12, 2000

Resonance-field dependence of signal intensity in electronically detected magnetic resonance (EDMR) has been investigated both theoretically and experimentally. Theoretical expressions presenting the field dependence of EDMR signal intensity are obtained from a quantum mechanical treatment of the Kaplan–Solomon–Mott model, where it is assumed that recombination only occurs through recombination pairs in the singlet spin state. In this study, effects of the exchange interaction in the recombination pair are explicitly taken into account. The resulting expressions show that the EDMR signal intensity is proportional to the square of the resonance field in a low-field region, whereas it becomes constant in a high-field region, which well explains literature experimental results. This paper also presents experimentally obtained variable-frequency (300–900 MHz) EDMR results for light-illuminated crystalline silicone. The experimental data have been analyzed in light of the present theoretical results, and the upper limit of the exchange interaction has been estimated.

Key Words: **EDMR; recombination; photoconductivity; silicon crystal; exchange interaction.**

INTRODUCTION

Electrically detected magnetic resonance (EDMR) is a version of electron spin resonance (ESR) which detects resonance signals as changes of conductivity. This method allows selective detection of defects and paramagnetic centers that are relevant to conductivity. Furthermore, its sensitivity has been shown to be much higher than that of conventional ESR (*1*). These advantages make this technique particularly suited to studies of semiconductor materials and devices, whose electric properties largely depend on the natures of recombination centers such as defects and paramagnetic centers. Numbers of materials and devices have so far been studied by EDMR, including not only varieties of Si samples such as plastically deformed Si (*2, 3*), amorphous hydrogenated Si (a-Si : H) (*4, 5*), and iron-contaminated Si (*6*), but also diverse devices such as Si diodes (*7–10*), p-i-n type solar cells (*11*), SiC and III–V semiconductor devices (*12*), and light-emitting diodes (*13, 14*).

One advantage of EDMR is that it observes changes in current or voltage. In general, detecting current or voltage is easier than detecting microwave absorption or dispersion, where the latter is made in usual ESR methods. Another advantage lies in the mechanism of recombination. In fact, it was a surprise in early studies that the intensities of observed EDMR signals are larger than that expected from a simple thermal equilibrium model (*1*). Kaplan, Solomon, and Mott (*15*) proposed a model (often referred to as the KSM model) which accounts for these unexpectedly large conductivity changes. The KSM model assumes that transient electron-hole pairs (or another type of spin–spin pairs depending on the type of recombination) are formed prior to the recombination and that the pairs should be in the singlet spin state for the recombination to proceed. Since the triplet–singlet spin conversion is not efficient under nonresonance conditions, the spin pairs in the triplet state will not participate in the recombination. When the system is brought to the resonance condition, on the other hand, the ESR transition induces the singlet–triplet conversion and thus the triplet spin pairs are allowed to participate in the recombination, which leads to an increase of the recombination rate. Kaplan *et al.* (*15*) formulated this model according to a classical treatment and demonstrated essential agreements between the theory and experimental results. A more rigorous and quantum-mechanics-based treatment was made by L'vov *et al.* (*3*). Their study confirmed the results of the classical treatment and demonstrated the validity of the KSM model. Recently, Lips *et al.* (*16*) investigated the KSM model more quantitatively and showed that the model reasonably explains the EDMR results of a-Si : H.

EDMR experiments have so far been performed with various microwave frequency-resonance field settings. These experiments have revealed that the intensity of the EDMR signal exhibits quite different field dependence from usual ESR. For example, Brandt *et al.* (*4*) performed EDMR experiments with microwave frequencies of $\nu = 0.434$, 9, and 34 GHz and concluded that the EDMR signal intensity (under microwave field of the same strength) does not depend on the microwave frequency employed. Barabanov *et al.* (*17*), on the other hand, examined much lower frequencies of 2–10 MHz and obtained different

[1] To whom correspondence should be addressed.

1090-7807/01 $35.00

type of field dependence, i.e., the EDMR signal intensity is approximately proportional to the square of the microwave frequency. We have recently performed an EDMR study with microwave frequencies in an intermediate range of 300–900 MHz (*18*). Our results reveal a saturation-type field dependence, where, although the EDMR signal intensity increases with the increase of the resonance field, the increasing rate decreases gradually. This finding strongly suggests that the two types of field dependence reported previously are in fact consistent with each other and that they only reflect the difference in the field range investigated.

The next subject would be to clarify the origin of this saturation-type field dependence, which is expected to provide valuable insight into further details of the mechanism of spin-dependent recombination. In this study, we attempt to derive theoretical expressions for EDMR which are applicable to a wide field range. In previous theoretical studies, a low-field or high-field approximation is often made, so that no reported equations seem to be applicable to both regions simultaneously. Furthermore, there is a notable discrepancy between the previous theoretical results (*3*) and our experimental results in field dependence of the linewidth of the EDMR signal. According to the theory by L'vov *et al.* (*3*), the splitting due to the g difference must exceed the (intrinsic) linewidth in the high-field region where the EDMR signal intensity is independent of the resonance field. Hence, one must observe a splitting of the EDMR signal or, more likely, inhomogeneous broadening due to g spread. This indeed applies well to their experimental results, which show an increase of the linewidth with the increase of the resonance field (*3*). On the contrary, this theoretical result does not accord with our experimental results, which show no evidence of such broadening (or splitting) (*18*). This discrepancy is most likely due to the fact that their theory does not explicitly include the exchange interaction that must be present in the transient spin–spin pair. Effects of the exchange interaction have been partly considered in previous studies (*19, 20*), and the presence of a small exchange interaction in the recombination pair has been expected. In this study, we formulate the effects of the exchange interaction on EDMR signal intensity according to the quantum mechanical spin density formalism. To our knowledge, this is the first EDMR theoretical study that presents a quantum mechanical spin-density-based treatment that explicitly includes the exchange interaction. This theoretical treatment has provided useful equations which well explain the saturation-type field dependence and enable an estimate of the strength of the exchange interaction.

THEORY

Preparations. In the KSM model, it is assumed that two spins form a transient pair prior to the recombination. As a matter of fact, there has long been controversy about the identities of the two spins, and this is correlated with the question of which step is most responsible for the spin dependence of the recombination (*5, 19–21*). For Si samples, it was shown that the tunneling from a band-tail state into a dangling-bond orbital dominates the recombination (*16*), and thus the two spins in the KSM model would be electron spins in the band-tail state and the dangling-bond orbital. Nevertheless, it should be noted that variations in the natures of the two spins do not affect the frame of the theory, but only influence the values of the parameters (*20*). Accordingly, in the theoretical formulation below, we do not specify the natures of the two spins.

We consider an exchange-coupled spin–spin pair, where one spin is denoted as $\mathbf{S}_\mathrm{e}$ and the other spin as $\mathbf{S}_\mathrm{h}$. When a static magnetic field B_0 is applied along the z axis and a microwave field B_1 is applied in the xy plane with an angular frequency of ω, the spin Hamiltonian H_spin for the spin–spin pair is

$$\begin{aligned} H_\mathrm{spin} &= H_0 + H_1; \\ H_0 &= -\hbar J \mathbf{S}_\mathrm{e}\cdot\mathbf{S}_\mathrm{h} + \left(g_\mathrm{e}\mu_\mathrm{B}S_\mathrm{e}^z + g_\mathrm{h}\mu_\mathrm{B}S_\mathrm{h}^z\right)B_0, \qquad [1] \\ H_1 &= g_\mathrm{e}\mu_\mathrm{B}B_1(S_\mathrm{e}^+e^{i\omega t} + S_\mathrm{e}^-e^{-i\omega t}) \\ &\quad + g_\mathrm{h}\mu_\mathrm{B}B_\mathrm{l}(S_\mathrm{h}^+e^{i\omega t} + S_\mathrm{h}^-e^{-i\omega t}), \qquad [2] \end{aligned}$$

where S_e^z and $S_\mathrm{e}^\pm(=S_\mathrm{e}^x \pm iS_\mathrm{e}^y)$ are spin components for $\mathbf{S}_\mathrm{e}$, and S_h^z and $S_\mathrm{h}^\pm(=S_\mathrm{h}^x \pm iS_\mathrm{h}^y)$ are components for $\mathbf{S}_\mathrm{h}$. The symbol J represents the exchange interaction parameter, g_e, and g_h represent the g values of the spin $\mathbf{S}_\mathrm{e}$ and $\mathbf{S}_\mathrm{h}$, respectively, and other symbols have their usual meanings. For later calculations, it is convenient to express the equations in the angular frequency unit as

$$\begin{aligned} H_0/\hbar &= -J\mathbf{S}_\mathrm{e}\cdot\mathbf{S}_\mathrm{h} + \omega_\mathrm{e}S_\mathrm{e}^z + \omega_\mathrm{h}S_\mathrm{h}^z, \qquad [3] \\ H_1/\hbar &= \eta_\mathrm{e}(S_\mathrm{e}^+e^{i\omega t} + S_\mathrm{e}^-e^{-i\omega t}) + \eta_\mathrm{h}(S_\mathrm{h}^+e^{i\omega t} + S_\mathrm{h}^-e^{-i\omega t}), \qquad [4] \end{aligned}$$

where $\omega_l = g_l\mu_\mathrm{B}B_0/\hbar$ and $\eta_l = g_l\mu_\mathrm{B}B_1/\hbar$ (l = e, h). In our experiments, the microwave field is not strong, so that we will treat H_1 as a perturbation. The matrix $H_0/\hbar$ can be readily solved and the following eigenenergies ω_j are obtained (*19, 20, 22*);

$$\begin{aligned} \omega_+ &= -J/4 + (\omega_\mathrm{e} + \omega_\mathrm{h})/2, \qquad [5\text{-}1] \\ \omega_\mathrm{a} &= J/4 + \kappa/2, \qquad [5\text{-}2] \\ \omega_\mathrm{b} &= J/4 - \kappa/2, \qquad [5\text{-}3] \\ \omega_- &= -J/4 - (\omega_\mathrm{e} + \omega_\mathrm{h})/2, \qquad [5\text{-}4] \end{aligned}$$

where

$$\begin{aligned} \kappa &= (J^2 + \Delta\omega^2)^{1/2}, \qquad [6\text{-}1] \\ \Delta\omega &= \omega_\mathrm{e} - \omega_\mathrm{h} = (g_\mathrm{e} - g_\mathrm{h})\mu_\mathrm{B}B_0/\hbar. \qquad [6\text{-}2] \end{aligned}$$

The eigenstates $|j\rangle$ expressed in terms of the bases for the total

spins, $|T_1\rangle$, $|T_0\rangle$, $|T_{-1}\rangle$, and $|S\rangle$, are as follows:

$$|+\rangle = |T_1\rangle, \quad [7\text{-}1]$$

$$|a\rangle = \alpha|S\rangle + \beta|T_0\rangle, \quad [7\text{-}2]$$

$$|b\rangle = \beta|S\rangle - \alpha|T_0\rangle, \quad [7\text{-}3]$$

$$|-\rangle = |T_{-1}\rangle, \quad [7\text{-}4]$$

where

$$\alpha = \mathrm{sgn}(\Delta\omega)[(\kappa - J)/(2\kappa)]^{1/2} \quad [8\text{-}1]$$

$$\beta = [(\kappa + J)/(2\kappa)]^{1/2}. \quad [8\text{-}2]$$

In order to relate quantum quantities with classical quantities, we must calculate the density matrix. For this calculation, it is convenient to take the rotating coordinate system which is rotating about the z axis at the angular frequency identical with that of the microwave field, ω. Then, using the new bases $|+\rangle' = e^{-i\omega t}|+\rangle$, $|a\rangle' = |a\rangle$, $|b\rangle' = |b\rangle$, and $|-\rangle' = e^{i\omega t}|-\rangle$, we have the following equation for the density matrix (*22*);

$$\frac{d\rho}{dt} = \frac{i}{\hbar}[\rho, H'_{\mathrm{spin}}] + \left(\frac{d\rho}{dt}\right)_{\mathrm{gen}} + \left(\frac{d\rho}{dt}\right)_{\mathrm{rec}} + \left(\frac{d\rho}{dt}\right)_{\mathrm{dis}} + \left(\frac{d\rho}{dt}\right)_{\mathrm{rel}}, \quad [9]$$

where H'_{spin} is the spin Hamiltonian expressed now in the rotating coordinate system. Its explicit form is given in Eq. [A1]. The second, third, fourth, and fifth terms on the right-hand side represent the changes of ρ due to the pair generation, electron-hole recombination, pair dissociation, and the spin relaxation, respectively (Fig. 1). These terms are taken as follows. First, the pair-generation term is taken as spin-independent as in literature studies (*3*, *15*):

$$(d\rho_{mn}/dt)_{\mathrm{gen}} = (r_g/4)\delta_{mn}. \quad [10]$$

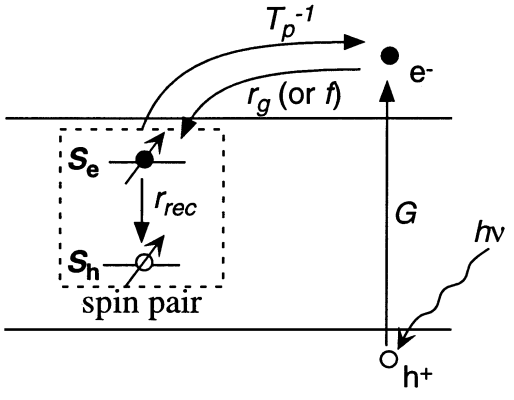

FIG. 1. Scheme of the recombination processes.

Second, we take the recombination term as

$$(d\rho_{mn}/dt)_{\mathrm{rec}} = -r_s\langle m|S\rangle\langle S|n\rangle\rho_{mn}, \quad [11]$$

where $|S\rangle$ is the pure singlet state, and r_s is the rate parameter for the recombination from the pure singlet state. It is clear from Eqs. [7] that $|a\rangle$ and $|b\rangle$ are the only eigenstates which have a nonzero product with $|S\rangle$, so that only the equations for ρ_{aa}, ρ_{bb} and $\rho_{ab} + \rho_{ba}$ have a nonzero recombination term. Third and last, the pair-dissociation term and the relaxation term are taken as

$$(d\rho_{mn}/dt)_{\mathrm{dis}} + (d\rho_{mn}/dt)_{\mathrm{rel}} = -\rho_{mn}/T_p \quad \text{for } m = n, \quad [12\text{-}1]$$

$$= -\rho_{mn}/T_2 \quad \text{for } m \neq n, \quad [12\text{-}2]$$

where T_p represents the lifetime of the pair and T_2 the well-known spin–spin relaxation time. Here we have omitted the spin–lattice relaxation term (T_1 term) to avoid unnecessary complexity (*23*). The spin–lattice relaxation time T_1 is usually in the order of 10^{-6} (*1*)–10^{-7} s (*2*), being much longer than typical values for the pair lifetime $T_p \sim 2.5 \times 10^{-8}$ (*16*)–5×10^{-8} s (*2*). Thus the pair will be dissociated before the spin state reaches its thermal equilibrium, which means that the effects of T_1 are not important here. Finally, collecting all the terms together, we can obtain the equations for the density matrix elements, which are shown in Eqs. [A2].

Recombination rate. On the basis of the above model, the recombination rate r_{rec} can be expressed in terms of density matrix elements as

$$r_{\mathrm{rec}} = r_s(\alpha^2\rho_{aa} + \beta^2\rho_{bb}). \quad [13]$$

Hence, our goal here is to deduce ρ_{aa} and ρ_{bb} from Eqs. [A2]. In order to do this, we take a perturbation approach by regarding $H_1/\hbar$ as a small perturbation (thus U_i's in Eqs. [A2] are small enough). With this approach, the nonperturbed density matrix elements (denoted ρ^0_{mn}) can be obtained using the steady-state approximation ($d\rho_{mn}/dt = 0$) as

$$\rho^0_{++} = \rho^0_{--} = r_g T_p/4, \quad [14\text{-}1]$$

$$\rho^0_{aa} = r_g T_p/\left[4\left(1 + \alpha^2 r_s^2 T_p\right)\right], \quad [14\text{-}2]$$

$$\rho^0_{bb} = r_g T_p/\left[4\left(1 + \beta^2 r_s^2 T_p\right)\right], \quad [14\text{-}3]$$

and $\rho^0_{mn} = (m \neq n)$. Next, we consider the changes of the density matrix elements induced by the spin resonance, $\Delta\rho_{mn}$ ($= \rho_{mn} - \rho^0_{mn}$), under the condition that these changes are small enough. Because of this condition, (1) we limit the terms to the second order of U_i, (2) we approximate the terms like $U_i^2\rho_{pm}$ as $U_i^2\rho^0_{mn}$, and (3) we ignore the small quantity $\eta_e - \eta_h$, which is proportional to $(g_e - g_h)B_1$, and thus we take $\eta \equiv \eta_e = \eta_h$. Furthermore, we assume that the separations of the relevant transitions are small enough or their intrinsic linewidth is large enough to have these transitions occur simultaneously

(i.e., all $\Delta\omega_{mn}$ appearing in Eqs. [A2] can be set at zero simultaneously). This approximation is based on the experimental fact that, as described below, we did not observe either a splitting or an inhomogeneous line broadening in the EDMR signal, which strongly suggests that the separations of the relevant transitions are smaller than their intrinsic linewidth in the field range. With these approximations, we obtain the following equations from Eqs. [A2]:

$$\left(T_{\mathrm{p}}^{-1}+\alpha^2 r_{\mathrm{s}}\right)\Delta\rho_{\mathrm{aa}}=4\beta^2\eta^2T_2\left(\rho_{++}^0+\rho_{--}^0-2\rho_{\mathrm{aa}}^0\right), \quad [15\text{-}1]$$

$$\left(T_{\mathrm{p}}^{-1}+\beta^2 r_{\mathrm{s}}\right)\Delta\rho_{\mathrm{bb}}=4\alpha^2\eta^2T_2\left(\rho_{++}^0+\rho_{--}^0-2\rho_{\mathrm{bb}}^0\right). \quad [15\text{-}2]$$

Substituting Eqs. [14] into Eqs. [15] yields a theoretical expression for the recombination rate r_{rec}. Since the resulting expression shows that r_{rec} is proportional to the pair-generation rate r_{g}, it is convenient to introduce a new quantity $k_{\mathrm{rec}}\equiv r_{\mathrm{rec}}/r_{\mathrm{g}}$. By use of this quantity, the following expressions are finally obtained:

$$r_{\mathrm{rec}}=k_{\mathrm{rec}}r_{\mathrm{g}}=\left(k_{\mathrm{rec}}^0+\Delta k_{\mathrm{rec}}\right)r_{\mathrm{g}}, \quad [16\text{-}1]$$

$$k_{\mathrm{rec}}^0=\frac{r_{\mathrm{s}}T_{\mathrm{p}}}{2}\cdot\frac{2J^2+(2+r_{\mathrm{s}}T_{\mathrm{p}})\Delta\omega^2}{4(1+r_{\mathrm{s}}T_{\mathrm{p}})J^2+(2+r_{\mathrm{s}}T_{\mathrm{p}})^2\Delta\omega^2}, \quad [16\text{-}2]$$

$$\Delta k_{\mathrm{rec}}=2\eta^2r_{\mathrm{s}}^2T_{\mathrm{p}}^3T_2\Delta\omega^2\frac{4J^2+(2+r_{\mathrm{s}}T_{\mathrm{p}})^2\Delta\omega^2}{\left[4(1+r_{\mathrm{s}}T_{\mathrm{p}})J^2+(2+r_{\mathrm{s}}T_{\mathrm{p}})^2\Delta\omega^2\right]^2}, \quad [16\text{-}3]$$

where k_{rec}^0 is the recombination rate (normalized by r_{g}) under nonresonance conditions and Δk_{rec} is the change of the recombination rate (normalized by r_{g}) induced by spin resonance. It is important to note that k_{rec}^0 and Δk_{rec} are independent of r_{g}. In Figs. 2 and 3, Eqs. [16-2] and [16-3] are respectively plotted versus $\Delta\omega/J$ for various $r_{\mathrm{s}}T_{\mathrm{p}}$, though, as shown later, only the curves for $r_{\mathrm{s}}T_{\mathrm{p}}<1$ will be relevant to actual systems. Figures 2a and 3a show that k_{rec}^0 and Δk_{rec} increase with the increase of $\Delta\omega/J$ for small $\Delta\omega/J$, and that, for $\Delta\omega/J\gg1$, they approach a constant value that is strongly dependent on $r_{\mathrm{s}}T_{\mathrm{p}}$. For k_{rec}^0, the value at $\Delta\omega/J=0$ is also dependent on $r_{\mathrm{s}}T_{\mathrm{p}}$, whereas the corresponding value for Δk_{rec} is invariably zero. In Figs. 2b and 3b, the curves for various $r_{\mathrm{s}}T_{\mathrm{p}}$ are normalized to have the same variation range. It is important to note that the shape of the curve does not change remarkably in the range $r_{\mathrm{s}}T_{\mathrm{p}}=0$–1 despite the wide variation of its scale.

Very small values have been reported toward the product $r_{\mathrm{s}}T_{\mathrm{p}}$ in actual systems. For example, r_{s} and T_{p} were estimated as $r_{\mathrm{s}}\sim2.5\times10^4\ \mathrm{s}^{-1}$ and $T_{\mathrm{p}}\sim5\times10^{-8}$ s for a plastically deformed Si (*2*), and $r_{\mathrm{s}}\sim10^4$–$10^6\ \mathrm{s}^{-1}$ (depending on defect density) and $T_{\mathrm{p}}\sim2.5\times10^{-8}$ s for undoped a-Si : H (*16*) (T_{p} in the present paper corresponds to $1/d$ in Ref. 16). These values give $r_{\mathrm{s}}T_{\mathrm{p}}\sim2.5\times10^{-4}$–$10^{-2}$. Hence, it is a good approximation to expand Eqs. [16-2] and [16-3] in terms of $r_{\mathrm{s}}T_{\mathrm{p}}$ and take only

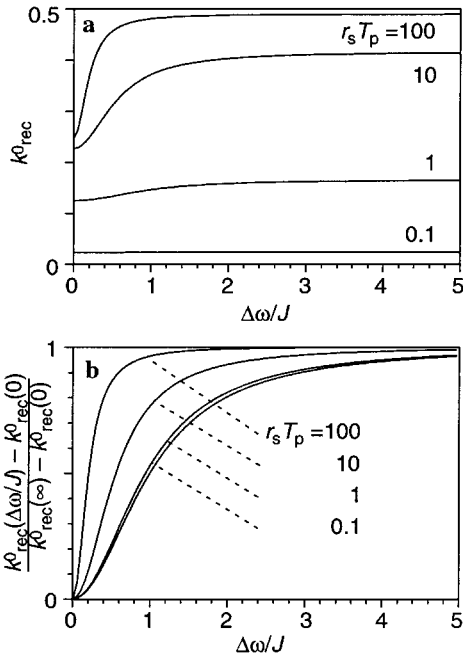

FIG. 2. Theoretically obtained dependence of the nonresonant spin-dependent recombination k_{rec}^0 on $\Delta\omega/J$ for $r_{\mathrm{s}}T_{\mathrm{p}}=0.1$, 1, 10, and 100. (a) $k^0{}_{\mathrm{rec}}-\Delta\omega/J$ curves in their original scales. (b) The same curves normalized with their respective variation ranges $|k^0{}_{\mathrm{rec}}(B_0=\infty)-k^0{}_{\mathrm{rec}}(B_0=0)|$.

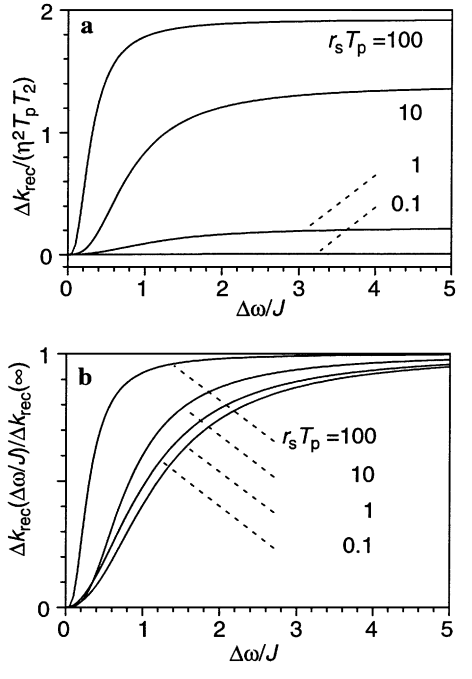

FIG. 3. Theoretically obtained dependence of the resonant spin-dependent recombination Δk_{rec} (equivalent to the EDMR signal intensity) on $\Delta\omega/J$ for $r_{\mathrm{s}}T_{\mathrm{p}}=0.1$, 1, 10, and 100. (a) $\Delta k_{\mathrm{rec}}/(\eta^2T_{\mathrm{p}}T_2)-\Delta\omega/J$ curves in their original scales. (b) The same curves normalized with their respective variation ranges $\Delta k_{\mathrm{rec}}(B_0=\infty)$.

small-order terms as

$$k_{\mathrm{rec}}^{0} = \frac{r_{\mathrm{s}}T_{\mathrm{p}}}{4} - (r_{\mathrm{s}}T_{\mathrm{p}})^{2}\frac{2J^{2}+\Delta\omega^{2}}{8(J^{2}+\Delta\omega^{2})} \qquad [17\text{-}1]$$

$$\Delta k_{\mathrm{rec}} = \frac{1}{2}\eta^{2}T_{\mathrm{p}}T_{2}\cdot(r_{\mathrm{s}}T_{\mathrm{p}})^{2}\frac{\Delta\omega^{2}}{J^{2}+\Delta\omega^{2}}. \qquad [17\text{-}2]$$

We will use these simplified equations instead of Eqs. [16-2] and[16-3] for further formulation below.

Conductivity. As a final process of the theoretical formulation, we will connect the recombination rate to the conductivity. Essentially following Lips *et al.* (*16*), we can obtain rate equations with respect to the conduction electron concentration n_{e} and the spin–spin pair concentration N as

$$dn_{\mathrm{e}}/dt = G - fn_{\mathrm{e}} + N/T_{\mathrm{p}}, \qquad [18\text{-}1]$$

$$dN/dt = fn_{\mathrm{e}} - N/T_{\mathrm{p}} - k_{\mathrm{rec}}fn_{\mathrm{e}}, \qquad [18\text{-}2]$$

where f is the coefficient for the pair-generation rate (i.e., $r_{\mathrm{g}} = fn_{\mathrm{e}}$), G is the generation rate of the conduction electron due to photoillumination (Fig. 1), and we have used our definition $r_{\mathrm{rec}} = k_{\mathrm{rec}}r_{\mathrm{g}}$ (see Eq. [16-1]). It should be noted that we do not need to distinguish the spin state of the pair because this effect is already included in k_{rec} in the above subsection. Equations [18] can be solved with the steady-state approximation as

$$n_{\mathrm{e}} = G/(fk_{\mathrm{rec}}). \qquad [19]$$

Since the conductivity is proportional to n_{e} and we have neglected the intrinsic carrier concentrations, we obtain

$$\sigma_{\mathrm{ph}} \propto {k_{\mathrm{rec}}}^{-1}. \qquad [20]$$

Consequently, the change of the photoconductivity $\Delta\sigma_{\mathrm{ph}}$ due to the microwave field is expressed as a ratio to the total photoconductivity σ_{ph} as

$$\begin{aligned}\Delta\sigma_{\mathrm{ph}}/\sigma_{\mathrm{ph}} &= -\Delta k_{\mathrm{rec}}/k_{\mathrm{rec}} \\ &= -2\eta^{2}T_{\mathrm{p}}T_{2}\cdot r_{\mathrm{s}}T_{\mathrm{p}}\cdot\Delta\omega^{2}/(J^{2}+\Delta\omega^{2}),\end{aligned} \qquad [21]$$

where we have used the actual relation $\Delta k_{\mathrm{rec}} \ll k_{\mathrm{rec}}$. Equation [21] predicts that $\Delta\sigma_{\mathrm{ph}}/\sigma_{\mathrm{ph}}$ is proportional to $\Delta\omega^{2}$ in the weak-field region ($\Delta\omega \ll J$), whereas it becomes constant in the strong-field region ($\Delta\omega \gg J$). The former behavior agrees with the EDMR results by Barabanov *et al.* (*17*), showing that the EDMR signal intensity is proportional to the square of the microwave frequency. The latter behavior, on the other hand, agrees with the results for higher microwave frequencies showing that the EDMR signal intensity is almost constant (*2–4*).

Quantitative consideration. Now we estimate Eqs. [17-1] and [17-2] and compare them with literature values as a test of the theory. The second term in Eq. [17-1] represents the field dependence of the recombination rate without microwave field, which is known as nonresonant spin-dependent recombination. Previous studies for a-Si (*24*, *25*) show that the magnitude of this effect is typically in the order of 10^{-3}–10^{-2} when expressed as a ratio to the total photoconductivity. From Eqs. [17-1] and [20], this ratio must be equal to or less than

$$|\sigma_{\mathrm{ph}}(B_{0}=\infty) - \sigma_{\mathrm{ph}}(B_{0}=0)|/\sigma_{\mathrm{ph}} = r_{\mathrm{s}}T_{\mathrm{p}}/2. \qquad [22]$$

Using the values reported by Lips *et al.* (*16*), $r_{\mathrm{s}} \sim 10^{4}$–$10^{6}$ s^{-1} (depending on defect density) and $T_{\mathrm{p}} \sim 2.5\times10^{-8}$ s, one can estimate the ratio as $\sim 1.25\times10^{-4}$–10^{-2}. This value is in agreement with the previous experimental results (*24*, *25*).

Equation [17-2], on the other hand, represents the change of the recombination rate due to application of microwave field, resonant spin-dependent recombination. The order of this effect as determined by EDMR is typically 10^{-5}–10^{-3} (*16*) when expressed as a ratio to the total photoconductivity. The expression for the ratio has been given in Eq. [21], and the maximum of the absolute value of the ratio is

$$|\Delta\sigma_{\mathrm{ph}}(B_{0}=\infty)/\sigma_{\mathrm{ph}}| = 2\eta^{2}T_{\mathrm{p}}T_{2}\cdot r_{\mathrm{s}}T_{\mathrm{p}}. \qquad [23]$$

Unfortunately, the magnitude of the microwave field B_{1} is usually not specified in literature papers, so that the $\eta^{2}T_{\mathrm{p}}T_{2}$ values in previous experiments are not clear. Therefore, here we use the value in our experiment ($B_{1} = 39.2\ \mu$T), which will not be very different from literature values. Then, also using the r_{s} and T_{p} values given above and $T_{2} = 2.6\times10^{-8}$ (from the linewidth $\Delta B_{\mathrm{pp}} \sim 0.25$ mT, see below), we can estimate $\eta_{2}T_{\mathrm{p}}T_{2} = 0.03$. This leads to an estimate of the ratio $\sim 1.5\times10^{-5}$–10^{-3}, which is again in agreement with the previous experimental results.

RESULTS AND DISCUSSION

In the previous study, we performed EDMR measurements for a light-illuminated *n*-type Si crystal in a frequency range 300–900 MHz (*18*). The study showed that the increase of the resonance field causes no changes in linewidth of the EDMR signal. In these measurements, however, we employed a relatively large amplitude of field modulation (0.4 mT) for the lock-in detection, which may have obscured a possible change of linewidth. We have therefore reinvestigated the field dependence of the EDMR signal using a smaller field modulation (0.13 mT). Representative spectra are shown in Fig. 4, where the upper panel (Fig. 4a) shows field-derivative spectra originally recorded on our apparatus and the lower panel (Fig. 4b) shows the numerical integrals of the field-derivative spectra. Figures 5 and 6 display the resonance-field dependence of the EMDR signal intensity and the peak-to-peak linewidth, respectively. The present results coincide with the previous ones within experimental errors. Important parameters are listed in Table 1, where some literature field-dependence EDMR data are also included for comparison.

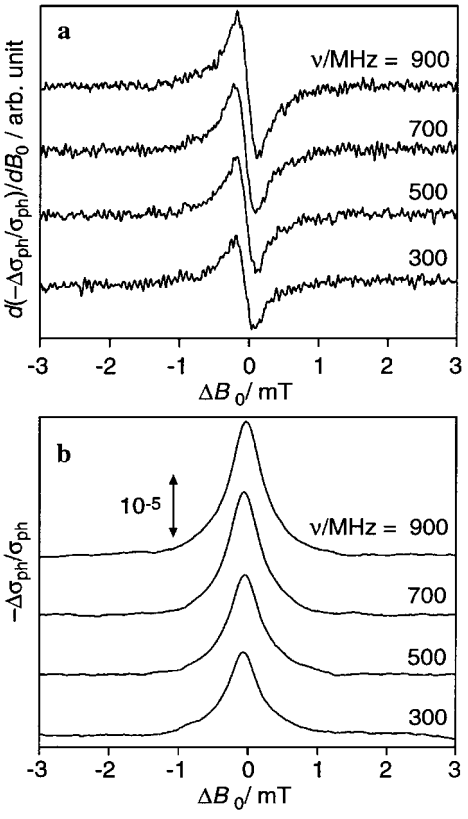

FIG. 4. EDMR spectra of a photoilluminated *n*-type Si crystal measured with microwave frequencies of $\nu = 300$, 500, 700, and 900 MHz. (a) Field-modulated spectra. Conditions: frequency and width of the field modulation, 365 Hz and 0.13 mT; field sweep rate, 10 mT/2.0 s, time constant, 1 ms; accumulation, 256 times; temperature, room temperature, $B_1 = 39.2\ \mu$T; bias current, 10 μA. (b) Numerical integrals of the spectra, where nonresonant effects appearing as a slanted baseline are subtracted.

As is clear from comparison between Figs. 3 and 5, the theoretical and experimental results exhibit the same field dependence. Thus one can estimate some parameters in the theory from the fitting of the data to Eq. [21]. A least-squares fit provides

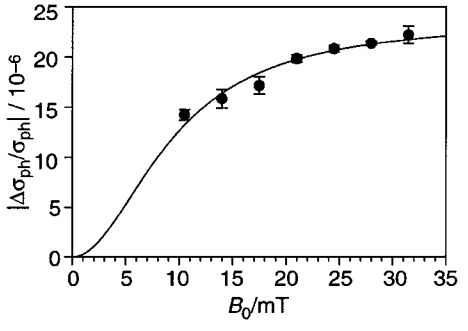

FIG. 5. Resonance-field dependence of the EDMR signal intensity. The solid circles represent experimental results for a photoilluminated *n*-type Si crystal at microwave frequencies of 300, 400, 500, 600, 700, 800, and 900 MHz. The bars represent the standard deviations from three independent recordings. Experimental conditions are given in the legend of Fig. 4. The solid curve is obtained from the least-squares fit to Eq. [21].

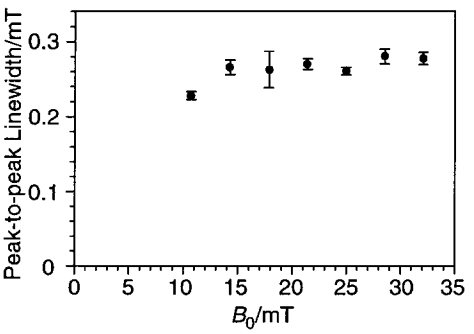

FIG. 6. Resonance-field dependence of the EDMR signal linewidth (the peak-to-peak linewidth). The solid circles represent experimental results for a photoilluminated *n*-type Si crystal at microwave frequencies of 300, 400, 500, 600, 700, 800, and 900 MHz. The bars represent the standard deviations from three independent recordings. Experimental conditions are given in the legend of Fig. 4.

$$\eta^2 T_p T_2 \cdot r_s T_p = 1.2 \times 10^{-5}, \qquad [24\text{-}1]$$

$$J/[2\pi \cdot |g_e - g_h|] = 1.3 \times 10^2 \text{ MHz}. \qquad [24\text{-}2]$$

Equation [24-1] can be used to estimate the recombination rate parameter for the pure singlet state, r_s. In our settings, $B_1 = 39.2\,\mu$T, which corresponds to $\eta = 2\pi \times 1.1 \times 10^6\ \text{s}^{-1}$. The spin–spin relaxation time may be estimated from the linewidth $\Delta B_{pp} \approx 0.28$ mT as $T_2 = 2.6 \times 10^{-8}$ s, where the relation $(g\mu_B/\hbar) \cdot \Delta B_{pp} = 2(3)^{-1/2} T_2^{-1}$ for the Lorentzian lineshape is used (*22*). Thus, also using $T_p = 2.5 \times 10^{-8}$ s (*16*), we obtain $r_s = 1.6 \times 10^4\ \text{s}^{-1}$. This value is reasonable for the recombination-rate parameter of the singlet state, compared well with literature values such as $2.5 \times 10^4\ \text{s}^{-1}$ (W_s in Ref. 2) and $10^4\ \text{s}^{-1}$ for Si of low defect density (*16*). Equation [24-2], on the other hand, can be used to estimate the exchange-interaction parameter J. To estimate J, however, we must know the difference of the g values. Unfortunately, the g difference is not clear from our data. Nevertheless, we can estimate its upper limit from the linewidth. The linewidth observed at $\nu = 900$ MHz is 0.28 mT (Fig. 6), from which we can estimated $|g_e - g_h| < 0.01$. We can therefore obtain $J/2\pi < 1.3$ MHz (*26*). This J value is smaller than the observed linewidth ($\sim$7 MHz in the frequency unit), which is consistent with the fact that we did not observe a splitting due to the exchange interaction. This J value is also in accordance with a previously estimated upper limit of $J < 30$ MHz (*20*). The magnitude of exchange interaction is strongly dependent on the distance between the two spins (*19*). Thus this relatively small J value seems to indicate that the two recombination centers are separated by a large distance.

In the theoretical study by L'vov *et al.* (*3*), the field dependence of the signal intensity was attributed to the change in the relation between $\Delta\omega$ ($\propto B_0$) and time parameters (which we may denote as T temporary). The time parameters include the spin relaxation times and the pair lifetime. According to their theory, the intensity of the EDMR signal increases with the increase of static field in the weak-field case ($\Delta\omega \ll 1/T$), whereas it

TABLE 1
Resonance-Field Dependence Data for EDMR of Silicone Samples

Sample	g Value	Microwave freq(GHz)	$\lvert\Delta\sigma_{ph}/\sigma_{ph}\rvert$ $(10^{-3})^a$	Linewidth (mT)^{a,b}	Temp (K)	Ref.
Single crystal	2.007 ± 0.002	9.3	0.001	1.5 (1/2)	300	1
Single crystal	2.005 ± 0.003	0.300–0.900	0.013–0.022 (@$B_1 = 39.2\,\mu$T)	~0.25 (pp)	RT[c]	This work
		0.890	0.041 (@saturation)		RT	18
Dislocated Si	NA[c]	0.005–0.009	0.09–0.24	~0.2 (1/2)	RT?	17
Deformed Si	NA	0.030	~0.02 (@saturation)	~0.2 (1/2)	300	3
		2.4	~0.1 (@saturation)	~0.8 (1/2)		
		9.4	~0.1 (@saturation)	~1.6 (1/2)		
a-Si : H	NA	0.434	~0.0015 (@$B_1 = 10\,\mu$T) ~0.01 (@saturation)	~0.2 (pp)	300	4
		9	~0.005 (@$B_1 = 10\,\mu$T) ~1 (@saturation)	~0.75 (pp)		
		34	~0.004 (@$B_1 = 10\,\mu$T)	~2.5 (pp)		

[a] Some values are directly read from figures.
[b] (1/2) indicates the full-width half-magnitude linewidth and (pp) indicates the peak-to-peak linewidth.
[c] NA, not available; RT, room temperature.

becomes constant in the strong-field case ($\Delta\omega \gg 1/T$). Since the time parameters determine the (intrinsic) linewidth of the signal, the strong-field case corresponds to the case where the g difference exceeds the linewidth. Hence, one can expect a splitting of the signal under high magnetic field. As a matter of fact, they did not observe such a peak splitting but a remarkable increase of the linewidth. They therefore concluded that a severe inhomogeneous line broadening due to g spread occurs in their system and that this obscures the expected splitting of the signal. In contrast to this, our sample showed no field-dependent changes in linewidth over the field range 10–35 mT (Fig. 4) despite the substantial change of the signal intensity. These results cannot be understood from the previous theory. On the contrary, these results are not surprising from the viewpoint of our theory because the field dependence of the signal intensity is due to the change in the relation between $\Delta\omega$ and J, not between $\Delta\omega$ and T. Interestingly, the T_2 value ($T_2 = 2.6 \times 10^{-8}$ s) estimated from the linewidth of our sample is comparable to the T_p value ($T_p = 2.5 \times 10^{-8}$ s). This strongly suggests that the observed linewidth comes mainly from the intrinsic linewidth and that there are no or negligible contributions from inhomogeneous line broadening at least in the field range <35 mT. Furthermore, as Table 1 shows, the smallest linewidths in previous variable-frequency EDMR studies are all around 0.2 mT, being very similar to the linewidth obtained in this study (~0.25 mT). This also supports the idea that $\Delta B = $ ~0.2–0.25 mT corresponds to the intrinsic linewidth.

EXPERIMENTAL

Variable-frequency EDMR measurements were performed on a spectrometer constructed in our laboratory. Briefly, the microwave generated by an Anritsu MG3633 oscillator and amplified by an R&K A1000-1050 power amplifier was led to a single-turn coil (8 mm in diameter), at the center of which a sample to be measured was placed. The magnetic flux density of the microwave field at the center of the coil was estimated using Eq. [3] in Ref. (*18*), and adjusted to a constant amplitude of $B_1 = 39.2\ \mu$T. The voltage between the two electrodes attached to the sample was measured with a PARC Model 5210 lock-in amplifier. The magnetic field was modulated at 365 Hz with a modulation coil for the lock-in detection. In this study, the amplitude of the field modulation was taken as 0.13 mT, which is smaller enough than the linewidth of the EDMR signal studied here. All the measurements were carried out at room temperature. The sample used was a rectangular-shape phosphor-doped n-type silicon crystal, where the phosphor concentration is ~10^{14}/cm^3 and the dark resistance is 5 kΩ-cm. The crystal had dimensions of 15 mm × 2 mm × 0.5 mm with the largest face being the (100) face. The crystal was illuminated with a light bulb (1 W) and given a bias current of 10 μA (which caused a voltage of ~0.693 V between the electrodes) during measurements. More details of our EDMR spectrometer and experimental setups were described previously (*18*).

APPENDIX 1

The spin Hamiltonian in the rotating coordinates is

$$H'_{spin}/\hbar = \begin{array}{c} \begin{matrix} |+\rangle' & |a\rangle' & |b\rangle' & |-\rangle' \end{matrix} \\ \begin{pmatrix} \omega_+ - \omega & U_1 & U_2 & 0 \\ U_1 & \omega_a & 0 & U_3 \\ U_2 & 0 & \omega_b & U_4 \\ 0 & U_3 & U_4 & \omega_- + \omega \end{pmatrix} \end{array}, \qquad [A1]$$

where

$$U_1 = Q\eta_e - P\eta_h, \qquad U_2 = P\eta_e + Q\eta_h,$$
$$U_3 = -P\eta_e + Q\eta_h, \quad U_4 = Q\eta_e + P\eta_h,$$

and

$$P = -\mathrm{sgn}(J)[(\kappa + \Delta\omega)/(2\kappa)]^{1/2},$$
$$Q = [(\kappa - \Delta\omega)/(2\kappa)]^{1/2}.$$

APPENDIX 2

The equation of the density matrix can be written as

$$d\rho_{++}/dt = -iU_1(\rho_{a+} - \rho_{+a}) - iU_2(\rho_{b+} - \rho_{+b}) - \rho_{++}/T_p + r_g/4, \quad [A2\text{-}1]$$

$$d\rho_{aa}/dt = iU_1(\rho_{a+} - \rho_{+a}) - iU_3(\rho_{-a} - \rho_{a-}) - \rho_{aa}/T_p - \alpha^2 r_s \rho_{aa} + r_g/4, \quad [A2\text{-}2]$$

$$d\rho_{bb}/dt = iU_2(\rho_{b+} - \rho_{+b}) - iU_4(\rho_{-b} - \rho_{b-}) - \rho_{bb}/T_p - \beta^2 r_s \rho_{bb} + r_g/4, \quad [A2\text{-}3]$$

$$d\rho_{--}/dt = iU_3(\rho_{-a} - \rho_{a-}) + iU_4(\rho_{-b} - \rho_{b-}) - \rho_{--}/T_p + r_g/4, \quad [A2\text{-}4]$$

$$d(\rho_{a+} - \rho_{+a})/dt = 2iU_1(\rho_{aa} - \rho_{++}) + iU_2(\rho_{ba} + \rho_{ab}) + i\Delta\omega_{+a}(\rho_{a+} + \rho_{+a}) - (\rho_{a+} - \rho_{+a})/T_2, \quad [A2\text{-}5]$$

$$d(\rho_{a+} + \rho_{+a})/dt = -iU_2(\rho_{ba} - \rho_{ab}) + i\Delta\omega_{+a}(\rho_{a+} - \rho_{+a}) - (\rho_{a+} + \rho_{+a})/T_2, \quad [A2\text{-}6]$$

$$d(\rho_{b+} - \rho_{+b})/dt = 2iU_2(\rho_{bb} - \rho_{++}) + iU_1(\rho_{ba} + \rho_{ab}) + i\Delta\omega_{+b}(\rho_{b+} + \rho_{+b}) - (\rho_{b+} - \rho_{+b})/T_2, \quad [A2\text{-}7]$$

$$d(\rho_{b+} + \rho_{+b})/dt = iU_1(\rho_{ba} - \rho_{ab}) + i\Delta\omega_{+b}(\rho_{b+} - \rho_{+b}) - (\rho_{b+} + \rho_{+b})/T_2, \quad [A2\text{-}8]$$

$$d(\rho_{ba} - \rho_{ab})/dt = iU_1(\rho_{b+} + \rho_{+b}) - iU_2(\rho_{a+} + \rho_{+a}) + iU_3(\rho_{-b} + \rho_{b-}) - iU_4(\rho_{-a} + \rho_{a-}) + i\omega_{ab}(\rho_{ba} + \rho_{ab}) - (\rho_{ba} - \rho_{ab})/T_2, \quad [A2\text{-}9]$$

$$d(\rho_{ba} + \rho_{ab})/dt = iU_1(\rho_{b+} - \rho_{+b}) + iU_2(\rho_{a+} - \rho_{+a}) - iU_3(\rho_{-b} - \rho_{b-}) - iU_4(\rho_{-a} - \rho_{a-}) + i\omega_{ab}(\rho_{ba} - \rho_{ab}) - (\rho_{ba} + \rho_{ab})/T_2 - \alpha\beta r_s(\rho_{ba} + \rho_{ab}), \quad [A2\text{-}10]$$

$$d(\rho_{-a} - \rho_{a-})/dt = 2iU_3(\rho_{--} - \rho_{aa}) - iU_4(\rho_{ba} + \rho_{ab}) + i\Delta\omega_{a-}(\rho_{-a} + \rho_{a-}) - (\rho_{-a} - \rho_{a-})/T_2, \quad [A2\text{-}11]$$

$$d(\rho_{-a} + \rho_{a-})/dt = -iU_4(\rho_{ba} - \rho_{ab}) + i\Delta\omega_{a-}(\rho_{-a} - \rho_{a-}) - (\rho_{-a} + \rho_{a-})/T_2, \quad [A2\text{-}12]$$

$$d(\rho_{-b} - \rho_{b-})/dt = 2iU_4(\rho_{--} - \rho_{bb}) - iU_3(\rho_{ba} + \rho_{ab}) + i\Delta\omega_{b-}(\rho_{-b} + \rho_{b-}) - (\rho_{-b} - \rho_{b-})/T_2, \quad [A2\text{-}13]$$

$$d(\rho_{-b} + \rho_{b-})/dt = iU_3(\rho_{ba} - \rho_{ab}) + i\Delta\omega_{b-}(\rho_{-b} - \rho_{b-}) - (\rho_{-b} + \rho_{b-})/T_2, \quad [A2\text{-}14]$$

where $\omega_{mn} = \omega_m - \omega_n$ and $\Delta\omega_{mn} = \omega_{mn} - \omega$. In the equations, the components ρ_{-+} and ρ_{+-} are omitted because they are not important when the single-quantum transitions $|+\rangle, |-\rangle \rightarrow |a\rangle, |b\rangle$ are concerned, as in this case.

REFERENCES

1. D. J. Lepine, *Phys. Rev. B* **6,** 436 (1972).
2. L. S. Mima, V. I. Strikha, and O. V. Tretyak, *Sov. Phys. Semicond.* **14,** 1328 (1980).
3. V. S. L'vov, L. S. Mima, and O. V. Tretyak, *Sov. Phys. JETP* **56,** 897 (1982).
4. M. S. Brandt, M. W. Bayerl, N. M. Reinacher, T. Wimbauer, and M. Stutzmann, *Mater. Sci. Forum* **258–263,** 963 (1997).
5. K. Lips, S. Schütte, and W. Fuhs, *Phil. Magn. B* **65,** 945 (1992).
6. T. Mchedlidze and K. Matsumoto, *J. Appl. Phys.* **83,** 4042 (1998).
7. I. Solomon, *Solid State Commun.* **20,** 215 (1976).
8. P. Christmann, W. Stadler, and B. K. Meyer, *Appl. Phys. Lett.* **66,** 1521 (1995).
9. Y. Kamigaki, T. Miyazaki, N. Yoshihiro, K. Watanabe, and K. Yokogawa, *J. Appl. Phys.* **84,** 2193 (1988).
10. T. Sato, H. Yokoyama, H. Ohya, and H. Kamada, *Rev. Sci. Instrum.* **71,** 486 (2000).
11. K. Lips and W. Fuhs, *J. Appl. Phys.* **74,** 3993 (1993).
12. N. M. Reinacher, M. S. Brandt, and M. Stutzmann, *Mater. Sci. Forum* **196–201,** 1915 (1995).
13. W. E. Carlos, E. R. Glaser, T. A. Kennedy, and S. Nakamura, *Appl. Phys. Lett.* **67,** 2376 (1995).
14. M. W. Bayerl, M. S. Brandt, and M. Stutzmann, *Phys. Stat. Sol. A* **159,** R5 (1997).
15. D. Kaplan, I. Solomon, and N. F. Mott, *J. Phys. (Paris)* **39,** L51 (1978).
16. K. Lips, C. Lerner, and W. Fuhs, *J. Non-Cryst. Solids* **198–200,** 267 (1996).
17. A. V. Barabanov, V. A. L'vov, and O. V. Tretyak, *in* "23rd International Conference on the Physics of Semiconductors," Vol. 4, pp. 2693–2696 (1996).
18. T. Sato, H. Yokoyama, H. Ohya, and H. Kamada, *J. Magn. Reson.* **139,** 422 (1999).
19. F. Boulitrop, *Phys. Rev. B* **28,** 6192 (1983).
20. F. C. Rong, W. R. Buchwald, E. H. Poindexter, W. L. Warren, and D. J. Keeble, *Solid.-State Electron.* **34,** 835 (1991).

21. B. C. Cavenett, S. P. Depinna, I. G. Austin, and T. M. Searle, *Phil. Magn. B* **48,** 169 (1983).

22. N. W. Atherton, "Principles of Electron Spin Resonance," Ellis Horwood, New York (1993).

23. Inclusion of the spin–lattice relaxation terms can be made in Eqs. [A2] by replacing T_p^{-1} and r_g with $T_p^{-1}+T_1^{-1}$ and $r_g+(\rho_{++}+\rho_{--}+\rho_{aa}+\rho_{bb})/T_1$, respectively, where it is assumed that the thermal equilibrium value of ρ_{mn} is equal to $(\rho_{++}+\rho_{--}+\rho_{aa}+\rho_{bb})/4$ for $m=+,-,$ a, b.

24. H. Mell, B. Movaghar, and L. Schweitzer, *Phys. Stat. Sol. B* **88,** 531 (1978).

25. M. Bhatnagar and I. Solomon, *in* "6th International Photovoltaic Science and Engineering Conference (PVSEC-6)," pp. 381–386 (1992).

26. The g difference between the band-tail electron ($g=2.0044$) and a dangling bond ($g=2.0055$) is reported as $\Delta g=0.0011$ (5). If this is the case in our sample, $J/2\pi \sim 0.14$ MHz can be obtained.